Research Article Vol. 32, No. 12 / 3 Jun 2024 / Optics Express 20491
Optics EXPRESS

Temporal variability in the relationship between line height absorption and chlorophyll concentration: a case study from the Northern Gulf of Alaska

Benjamin Lowin,[1] Suzanne Strom,[2] William Burt,[3] Thomas Kelly,[4] and Sara Rivero-Calle[1,*]

[1]*Skidaway Institute of Oceanography and Department of Marine Sciences, University of Georgia, 10 Ocean Science Circle, Savannah, GA 31411, USA*
[2]*Shannon Point Marine Center, Western Washington University, Anacortes, WA 98221, USA*
[3]*Planetary Technologies, Halifax, Canada*
[4]*College of Fisheries and Ocean Sciences, University of Alaska Fairbanks, Fairbanks, AK 99775, USA*
[*]*rivero@uga.edu*

Abstract: The Line Height Absorption (LHA) method uses absorption of light to estimate chlorophyll-a. While most users consider regional variability and apply corrections, the effect of temporal variability is typically not explored. The Northern Gulf of Alaska (NGA) was selected for this study because there was no published regional value and its large swings in temporal productivity would make it a good candidate to evaluate the effect of temporal variability on the relationship. The mean NGA value of 0.0114 obtained here should be treated with caution, as variation in the slope of the relationship (a_{LH}*), and thus chlorophyll-a estimates, in the NGA region varied by ~25% between spring (a_{LH}* = 0.0109) and summer (a_{LH}* = 0.0137). Results suggest that this change is driven by a shift in pigment packaging and cell size associated with changes in mixed layer depth and stratification. Consideration of how temporal variability may affect the accuracy of the LHA method in other regions is thus recommended.

1. Introduction

Understanding the amount of phytoplankton biomass in the world's oceans is critical for the sustainable management of fisheries and constraining the Earth's carbon cycle. To do this, historical work has relied on the connection between phytoplankton biomass and chlorophyll-a concentrations. Several methods exist to derive chlorophyll-a concentrations from absorption, including line height absorption (LHA) [1], remote sensing band ratios [2], and peak height (a similar method without accounting for the baseline) [3]. The LHA method is becoming more popular as it accounts for the effect of accessory pigments, is unaffected by non-photochemical quenching and mitigates the effect of Colored Dissolved Organic Matter (CDOM). The LHA method is robust as it can be applied in a wide range of environments and instrumental setups. It works well in optically complex waters, such as the South China Sea [4], off the coast of British Columbia [5], and in the Gulf of Maine [1]. It has been employed on underway systems [5,6], with discrete niskin samples [4], with autonomous profilers including the Wetlabs Thetis profiler [7] and Argo floats [8,9], and with remote sensing data [10,11].

The LHA method makes use of the absorption of light at 676 nm to estimate chlorophyll-a concentration [1]. To implement the method, a baseline (representing the absorption slope without chlorophyll-a present) is calculated by drawing a straight line between the absorption values of 650 nm and 715 nm. The height of the 676 nm absorption peak is then measured from this baseline, known as the absorption line height (a_{LH}). A relationship between a_{LH} and chlorophyll-a is then calculated as the slope of a linear relationship between the a_{LH} measurements and *in*

#521758 https://doi.org/10.1364/OE.521758
Journal © 2024 Received 27 Feb 2024; revised 3 May 2024; accepted 6 May 2024; published 20 May 2024

Optics EXPRESS

situ chlorophyll-a readings. This approach is known as the chlorophyll-a-specific absorption line height (a_{LH}*). This linear algorithm is theoretically invariant to CDOM concentrations, accessory pigment composition, and most water qualities; however, chlorophyll-a pigment packaging has been shown to impact line height absorption by introducing non-linearities at low chlorophyll-a concentrations. Previous studies that have shown such an effect found it to yield a small uncertainty in chlorophyll-a concentrations [12–14].

The original work [1] demonstrated that a_{LH}* was variable between four study sites and attributed these changes to variations in pigment packaging effects. A follow-up meta-analysis confirmed that a_{LH}* widely ranges in the global oceans [12] with reported values between 0.0054 and 0.0250 m^2 ug^{-1}. This is around a mean value of 0.0108 m^2 ug^{-1} with 25th and 75th quartile bounds of 0.0073 and 0.0149, respectively. Therefore, regionally tuning a_{LH}* values has become common when using the LHA method, but the effect of temporal variability on a_{LH}* at a given site has not been addressed. Moreover, a regional value for the Northern Gulf of Alaska (NGA) has not been reported.

The NGA is a high-latitude region with an intense seasonal cycle of primary production and chlorophyll-a biomass [1,15–18]. Light limitation during the winter alternates with summer nutrient limitation, leading to a boom-bust cycle that results in a large range in chlorophyll-a concentration and phytoplankton community composition. This variability makes the NGA a suitable region to determine to what degree a_{LH}* is temporally variable. Here we present a case study using the NGA to demonstrate the effect of temporal variability on a_{LH}*. To evaluate this potential, we deployed an optical inline system on the R/V Sikuliaq for two years across four deployments.

2. Methods

2.1. Site description

The data were collected from the R/V Sikuliaq on 4 cruises. These took place in the summer (June) 2020, fall (September) 2020, spring (April) 2021, and summer (July) 2021. These cruises were part of the NGA Long Term Ecological Research (LTER) program. The ship transited the whole NGA region, from Kodiak Island to the mouth of the Copper River and into Icy Bay in Prince William Sound (Fig. 1). The ship also transited the historical Seward Line, which has been sampled regularly for more than 25 years.

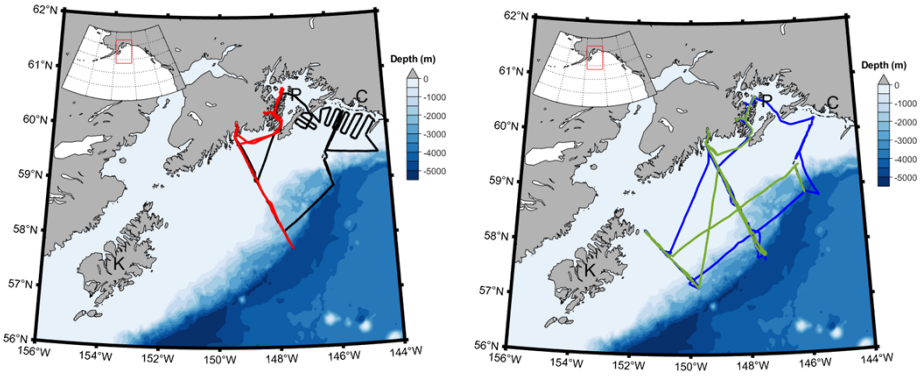

Fig. 1. Maps of the NGA showing the four cruise tracks and the bathymetry of the region. The line colors represent different cruises; black – Summer 2020, red – Fall 2020, blue – Spring 2021, and green – Summer 2021. The location of Kodiak Island (K), Prince William's Sound (P) and the Copper River (C) are marked on both maps.

Optics EXPRESS

2.2. Inline system

An optical inline system was deployed in parallel to the R/V Sikuliaq's standard inline system. The design of this system follows previously published work [5]. Briefly, the system was comprised of a Sea-Bird ACS measuring absorption (a) and attenuation (c) and a Sea-Bird Eco-triplet (BB3). Only the ACS data are used in this paper. The system was equipped with an automated three-way valve that caused the seawater to be diverted through a series of filters (a 1 µm filter followed by a 0.2 µm filter) to measure particulate blanks for 10 min of every hour. The blank period was 10 minutes so the reading became stable. The inline system was calibrated with distilled water (DI water) at the start and end of the cruise. DI water values were the same at both points in time.

2.3. Discrete samples

Over the course of the cruise, discrete water samples were taken from both conductivity temperature and depth (CTD) casts and the inline system to measure chlorophyll-a concentrations. The CTD rosette samples were taken at the surface (2 m depth) and 10 m depth. The intake for the inline water system is 6 m below the water surface. The chlorophyll-a samples were filtered on board using a vacuum pump and stacked filtration. The stacked filtration used two filters, one polycarbonate filter (47 mm diameter, pore size 20 µm) and one Whatman GF/F filter (25 mm diameter, nominal pore size 0.7 µm). Stacked filtration was used to estimate chlorophyll-a concentrations in both small (<20 µm) and large (>20 µm) phytoplankton size groups. Samples were analyzed on board with a Turner AU-10 benchtop fluorometer using the acidification method following a 24-h (dark, -20°C) 90% acetone extraction [19].

All data from the CTD rosette are processed and published online as part of the NGA LTER program [20]. We used 1m-binned photosynthetically available radiation (PAR) and density profiles from the CTD rosette to calculate median profiles for each cruise (i.e., sampling season). Further we calculated the mixed layer depth based on a threshold increase of 0.01 and 0.05 kg m^{-3} from the 2 m depth bin [21]. We also calculated the diffuse attenuation coefficient from the PAR data following Eq. (1),

$$Kd = \frac{1}{z}\ln\left(\frac{E_o}{E_z}\right), \tag{1}$$

where E_o is the surface irradiance and E_z is the 12 m irradiance. We only used stations that had a $E_0 > 200$ µmol/m^2/s to remove the effect of high cloud cover or low light conditions on the data.

2.4. ACS data processing

The ACS data were processed following a modified version of Burt *et al*. [5], using MATLAB (2022b, MathWorks, Natick, MA, USA). The code used for processing is publicly available on GitHub (https://github.com/Ben-Lowin/Ocean_optics_GOA.git). A brief description of the processing steps is as follows. The ACS data were averaged per second, then the ACS and BB3 data were aligned using blank periods as a reference to adjust for the temporal offset caused by instrument order. Next, the Sullivan correction for residual temperature and salinity was applied to the data [22]. The data were then averaged to one-minute bins for alignment with R/V Sikuliaq's inline system and trimmed around start and stop periods. Bad data (i.e., bad blanks, bubble spikes, high noise and drift) were flagged and removed from further processing. Flag data was less than one percent of data for all cruises. A correction for spectral discontinuity was applied, along with a center band correction to account for the change between the absorption and attenuation sensor bands, following the manufacturer's guidelines and the IOCCG (International Ocean Color Coordinating Group) protocol series [23,24]. The particulate absorption was then calculated from the processed ACS data. This calculation was done by subtracting a dissolved absorption spectrum, measured using filtered seawater (pore size 0.2 µm), from the total absorption spectra.

Optics EXPRESS

The dissolved absorption spectra were obtained by linear interpolation between the lowest total absorption values from each filter period, to make an equivalent 1-minute binned dissolved absorption data set.

2.5. Chlorophyll-a calculations

The particulate absorption spectra were used to determine chlorophyll-a concentration estimates following Roesler and Barnard [1]. First the baseline absorption value (a_{BL}) is calculated with,

$$a_{BL}(\lambda_{ref}) = \frac{a(715) - a(650)}{715 - 650} \cdot (\lambda_{ref} - 650) + a(650) \quad (2)$$

where a(λ) is the absorption at a given wavelength. The λ_{ref} for this is 676 nm, which is where there is an absorption peak for chlorophyll-a. This baseline is then used to calculate the absorption line height (a_{LH}) with,

$$a_{LH}(676) = a(676) - a_{BL}(676) \quad (3)$$

The a_{LH} values are then compared against discrete samples to determine the chlorophyll-a-specific absorption (a_{LH}*) (e.i., the slope of the relationship). This is done by a linear regression with the following equation;

$$Chl = a_{LH}^{*} \cdot a_{LH}(676) + b \quad (4)$$

The a_{LH} values were averaged for 10 minutes on either side of a station and plotted against total discrete chlorophyll-a sample estimates. The discrete sampling of chlorophyll-a concentration occurred at either the surface (approximately at 2 m depth) or at 10 m depth, which is different from the R/V Sikuliaq's seawater intake (at 6 m depth). To determine which of the two depths should be used to compare the discrete vs. a_{LH}-derived chlorophyll-a, both data sets were analyzed using linear regressions. The surface chlorophyll-a had a much better relationship with LHA ($r^2 = 0.92$) than the 10 m depth chlorophyll-a ($r^2 = 0.72$). Therefore, the rest of the analysis was done using the surface data.

As pigment packaging effects can cause the relationship between chlorophyll-a and absorption to be non-linear, particularly at lower chlorophyll-a concentrations, a power function fit has been suggested as a better approach [12]. Therefore, a power function fit was also explored for completeness but the results of this analysis show only slightly better R^2 values, a mean increase of 0.005 (see Supplement 1). Since neither our results nor those of the proponents of such method [12] found a meaningful increase in fit between these two relationships, and the scientific community is solely using the linear relationship, our work will focus on investigating the temporal variability using the linear relationship.

Since our data was non-parametric, a traditional linear regression is not appropriate but statistical bootstrapping methods can be used to solve this problem, estimate the slope and include an uncertainty estimate. The data sets were bootstrapped 1000 times, using the 2022b version of MATLAB's *bootstrp* function followed by the *fitlm* function that performed a linear regression by iteratively reweighting a least squares algorithm. The *fitlm* function used Eq. (4) as its base and allowed both a_{LH}* and b to vary following Roesler and Barnard (2013) who allowed both to vary. The *fitlm* function estimates the median and variance in the slope, and the standard error was then calculated based on the bootstrapped values.

3. Results

The cruises in the NGA took place over two years. Cruise tracks covered very similar water (Fig. 1), with a few exceptions. To determine if the change in sampling was driving a change we looked at the a_{LH}* with and without the different regions. The summer 2020 cruise also included an extensive study of the Copper River Plume (CRP) a freshwater dominated region of the NGA; this summer cruise added the grid pattern that can be seen in the northeast. To determine if the

Optics EXPRESS

CRP data affected the a_{LH}* relationship, we removed the additional three samples associated with this track and re-did a non-bootstrapped linear regression. Comparing a_{LH}* with and without the CRP resulted in 0.01256 ± 0.0005 and 0.01252 ± 0.0005 respectively, where the ± refers to the 95% CI of the slope. This shows that there is no significant difference in a_{LH}* with and without the CRP section; accordingly, the CRP section of the cruise was retained in the analysis.

The spring 2021 and summer 2021 cruises also included a region to the southwest known as the Kodiak line (Fig. 1) (see Supplement 1). We did the same analysis to this region. Comparing a_{LH}* with and without the Kodiak line for spring 2021 showed 0.01081 ± 0.0005 and 0.01046 ± 0.0007 respectively, where the ± refers to the 95% CI of the slope. Comparing a_{LH}* with and without the Kodiak line for summer 2021 showed 0.01363 ± 0.0007 and 0.01449 ± 0.0013 respectively, where the ± refers to the 95% CI of the slope. This indicates that the inclusion of the Kodiak line is weakening the relationship between chlorophyll-a and a_{LH}*, this is expected as the Kodiak line is known to have a different seasonality and community than the Seward line due to bathymetric mixing. While removal of this region would strengthen the temporal trend, it significantly reduces the sample size from ~30 to ~20. We chose to be conservative and include the Kodiak line in the rest of the analysis as it makes the analysis applicable to the whole NGA region.

All cruise tracks crossed multiple fronts. The most noticeable was the transition from the shelf to the offshore High Nutrients Low Chlorophyll-a (HNLC) region. This transition can be seen as a low chlorophyll-a region on all cruise tracks (Fig. 2 – green sections). When passing in and out of the HNLC region, the LHA method was able to see the rapid change in chlorophyll-a from 0.2 µg/l to 1.6 µg/l in the span of 20 minutes (approximately 6 km) in fall 2020 (start of green section on Fig. 2(A)). Similar changes in chlorophyll-a were seen on all cruises. Spring 2021 had such a large spring bloom that traveling through the transition resulted in a change of 10.5 µg/L. These substantial changes were also captured in the discrete samples.

In addition to the inline system optical data, density and PAR profiles were collected and the median values for each sampling season were calculated (Fig. 3). Our analysis focused on the top 12 m of the water column where the discrete samples and inline data were obtained. The density profiles show that fall 2020 was the least dense and spring 2021 was the densest (Fig. 3(A)). Further analysis of the density fields was done to determine the mixed layer depth (MLD) for a 0.01 (and 0.05) kg m^{-3} change in density at each station and the median value was calculated for each cruise [21]. This found Spring 2021 to have the deepest MLD of 10 m (14 m), then summer 2021 at 6.5 m (10 m), fall 2020 at 6 m (9 m) and summer 2020 at 5 m (4 m). Based on the MLD, Spring 2021 was the least stratified, and fall 2020 was the most stratified, showing a mixed layer to five meters in depth. Regarding the PAR data, fall 2020 had the lowest median surface value, and summer 2020 had the highest (Fig. 3(B)). Furthermore, the diffuse attenuation coefficients were 0.1929, 0.1983, 0.2434, 0.3118 for summer 2020, fall 2020, spring 2021 and summer 2021, respectively. This analysis suggests that summer 2020 was the clearest water and summer 2021 was the fastest attenuating.

To explore seasonal variability in a_{LH}*, the slopes of linear regressions between a_{LH} and chlorophyll-a were calculated for each cruise (Fig. 4). As explained in the methods, the regressions were bootstrapped to estimate uncertainty and to mitigate issues stemming from violations of the assumptions for a standard linear regression. All the regressions showed a strong relationship between a_{LH} and chlorophyll-a, with r^2 values equal to or greater than 0.885 and p-values < 0.001. The lowest r^2 is from fall 2020, which may be related to the lower n of 18, compared to the other cruises that have n closer to 30. To evaluate if the y-intercept is close to zero, standard error was used. This showed that values were close to but not zero. The whole dataset had an average a_{LH}* of $0.0114 \pm 0.0002\ m^{-1}$; however, a_{LH}* varied seasonally (Fig. 4 and 5(A)). a_{LH}* values were higher during the summer months than in the fall or spring. The bootstrapped standard error around a_{LH}* does not overlap between any of the cruises.

Optics EXPRESS

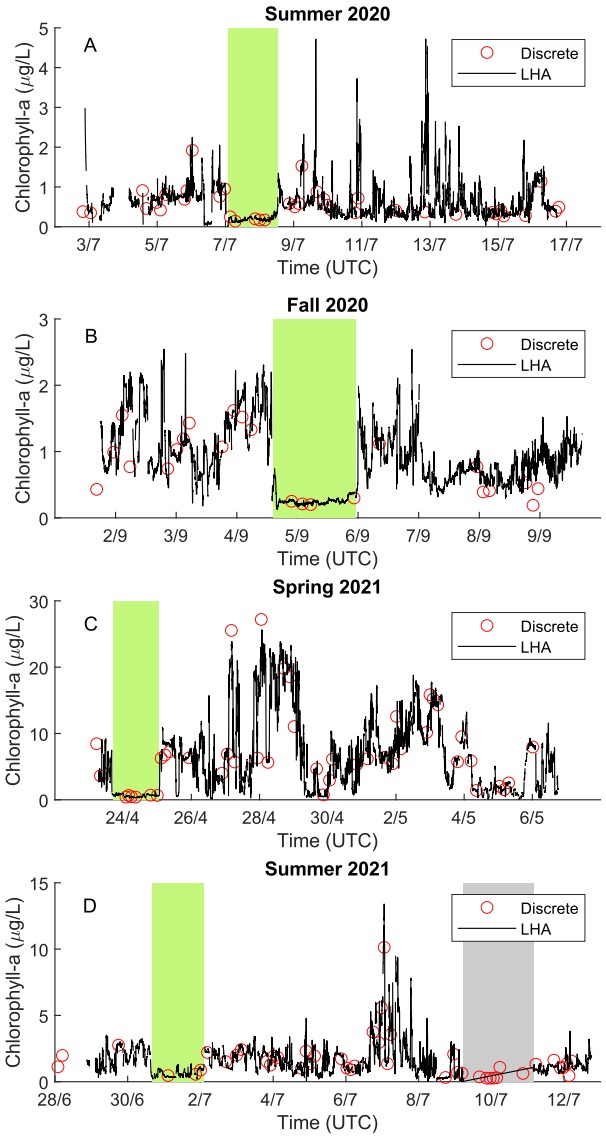

Fig. 2. Cruise timeseries for the summer 2020 (A), fall 2020 (B), spring 2021 (C), and summer 2021 (D). The black lines show the optically-derived chlorophyll and the red circles show total chlorophyll-a from discrete samples. The green sections indicate the HNLC regions. The grey box in D indicates a period of missing ACS data.

Optics EXPRESS

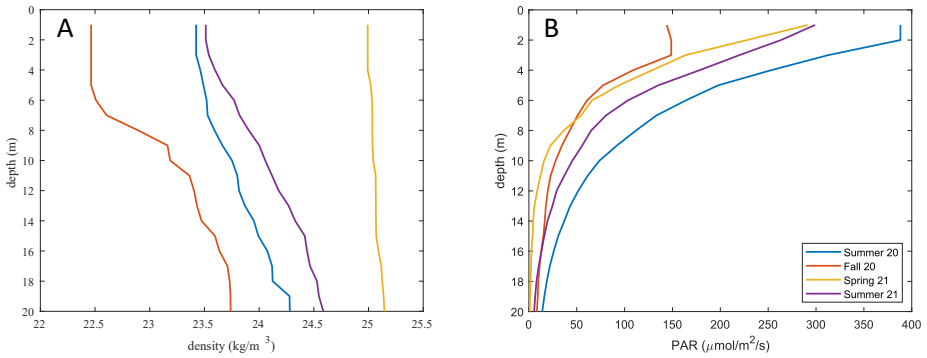

Fig. 3. Median density (A) and Photosynthetically Available Radiation (B) from CTD casts for each cruise. The legend is the same for both A and B.

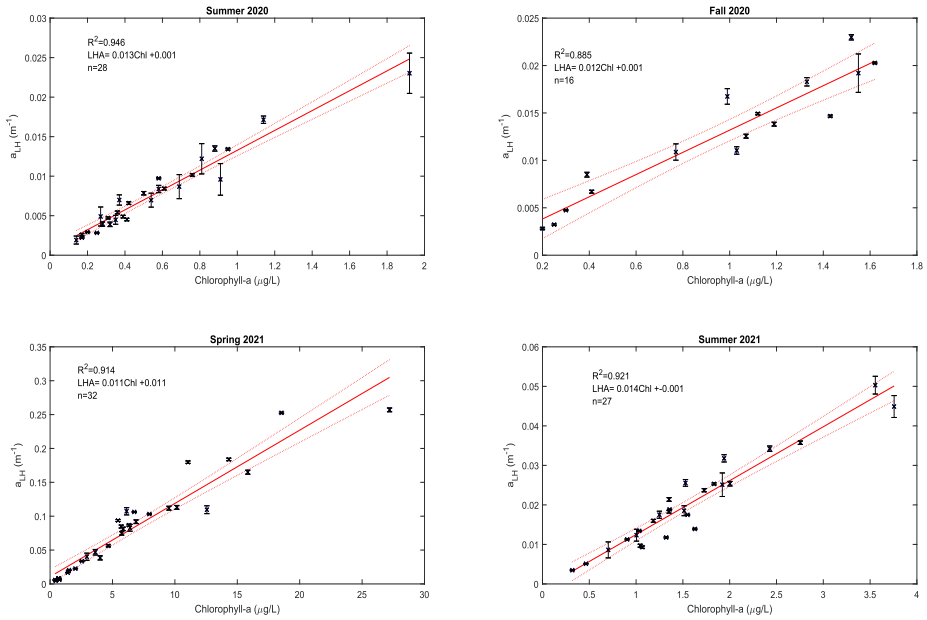

Fig. 4. Comparison between discrete chlorophyll-a samples at the surface and a_{Lh} for each station for each cruise. The red line is the linear regression with the dashed lines showing the 95% confidence interval of the regression. The error bars show the standard deviation around the mean value of the 20 mins of a_{Lh} data.

The dramatic increase of a_{LH}* values in the spring 2021 data corresponds with an exceptionally large spring bloom (Fig. 4(C)). Some of our discrete chlorophyll-a-a measurements during that period exceeded 25 µg/L (Fig. 2(C)). A large portion of the discrete samples was visually inspected under the microscope (not shown here), confirming that this spring bloom comprised a mixture of chain diatoms and colonial *Phaeocystis*. This community composition was different from the small phytoplankton that were seen in the summer 2020 and fall 2020 cruises (also determined from microscopy work). The size-fractionated chlorophyll-a data allowed us to investigate further the effects of this difference in community composition.

To understand whether the seasonal change in a_{LH}* was linked to a change in the size of the phytoplankton, we compared the proportion of chlorophyll-a attributed to small cells (<20 µm;

Optics EXPRESS

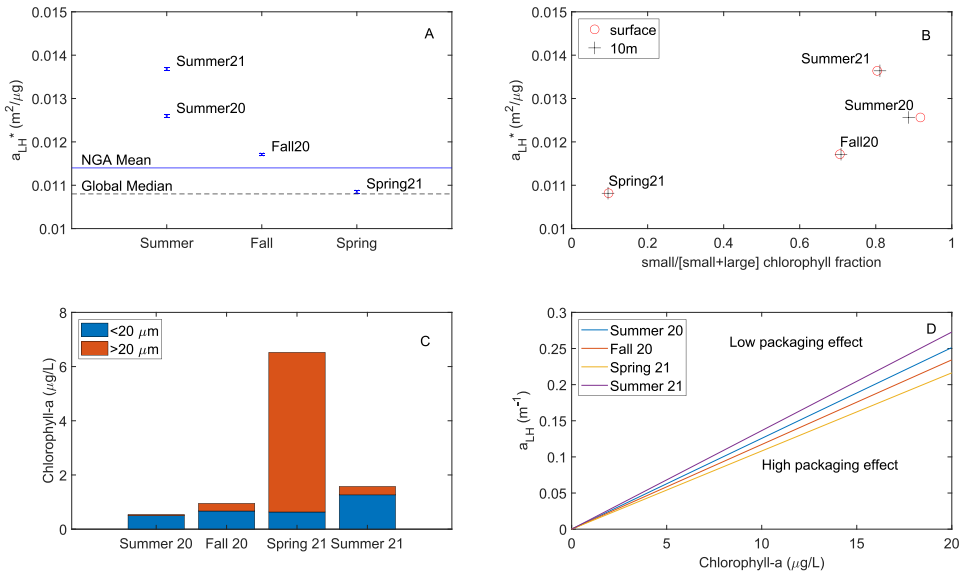

Fig. 5. A- Comparison of the a_{LH}* values for each cruise. The error bars show bootstrapped standard error. For reference, the global median value of 0.0108 [1,12] and the NGA mean value of 0.0114 are shown. B- F_{small} chlorophyll fraction compared to a_{LH}* across the 4 cruises. The red circles are at the surface and the black crosses are from 10 m data. C- The median contribution of small and large phytoplankton size fractions to total median chlorophyll for each cruise. D- Schematic showing how the packaging effect might explain the change in a_{LH}*.

herein referred to as F_{small}) to the a_{LH}*(Fig. 5(B)). Our data indicate a trend where low F_{small} is associated with a low a_{LH}*. Both summers have a high F_{small} and high a_{LH}*, but there is a difference between the summer values. Therefore, we investigated whether this difference between the two summer periods could be due to the depth of the MLD when the samples were taken. Indeed, the median MLD of summer 2021 was 6.5 m compared to 5 m in summer 2020. This 1.5 m change represents the loss of approximately 20% of surface irradiance from summer 2020 to summer 2021 (Fig. 3(B)). This would impact the amount of light available for phytoplankton, and thus the degree of pigment packaging present in cells. The F_{small} data also suggests that differences in water column stratification played a role in the summer differences in a_{LH}*. In general, the fraction of chlorophyll-a in nano- and pico-sized cells (F_{small}) did not change much between the 2 m and 10 m sampling depths (Fig. 5(B)) but in the summer 2020 cruise there is a change in F_{small} from 0.917 (at 2 m) to 0.886 (at 10 m). This change between the two depths is more evident in total chlorophyll-a: in summer 2021 there is a small difference in chlorophyll-a concentration of 0.02 µg/L between the two depths, whereas in summer 2020 the difference increases by an order of magnitude to 0.2 µg/L.

4. Discussion

Our results show that the LHA method provides accurate chlorophyll-a concentrations across various waters types within the NGA, including oligotrophic waters, eutrophic coastal waters, estuarine glacial waters, and river plumes (Fig. 2). To the best of our knowledge, this dataset is the first time that the LHA method has been deployed in seawater with glacial flour (2-65 µm in size), which is important because glacial flour has been shown to impact both absorption and attenuation [25]. The results shown here suggest that the LHA method is robust to glacial flour

Optics EXPRESS

effects, as the baseline subtraction removes the effect when estimating chlorophyll-a. Nonetheless, cleaning the optical system after passing through such an environment is recommended as the fine, lithogenic particles quickly settle.

Understanding how temporal variability affects the a_{LH}* is important for achieving high accuracy with the LHA method. The values that we found across the different seasons fall within the expected global range of 0.00006 to 0.0944 for a_{LH}* values [12] and our average value of 0.0114 for a_{LH}* is close to the global median value of 0.0108. As a reminder, the global value has a 25th and 75th quartile bounds of 0.0073 and 0.0149, respectively. The NGA values extend from 0.011 to 0.014, with a resulting range of 0.003, which represents a small variability in terms of the global values. Comparing with previous studies, the a_{LH}* values in the NGA look like other high latitude coastal regions and open ocean regions. The spring 2021 value is close to the values found for the Gulf of Maine (0.014) [1], the St. Laurence River (0.014) [26], and East Sound in Washington State (0.014) [27]. These are all high productivity, high latitude regions. In comparison the summer 2020 data looks like values found from BIOSOPE in the South Pacific (0.011) [12], GASEX in the South Atlantic (0.011) [12] and Long Island Sound (0.011) [12]. Two of these are open ocean data sets, and the Long Island Sound data comes from May and June, summer months. This suggests that the NGA is more similar to high latitude coastal regions in the spring and offshore environments in the summer.

Using the NGA average value in place of the seasonal values would lead to a 5.5% and a 19.2% deviation in chlorophyll-a estimates for our minimum and maximum values, respectively. Furthermore, if we were to apply the spring 2021 value to the summer 2021 data set, there would be a 26.1% error in chlorophyll-a estimates. Our data show that the NGA has a clear temporal variability to the a_{LH}*.

Based on our data, this variability is driven by a change in the pigment packaging and community composition. The change in packaging is driven by a mixture of changes in cell size, chlorophyll-a concentrations, community composition, and variation in photoacclimation [12]. We think that all of these came into play in the NGA, but our data only allow consideration of the cell size in two relatively coarse size fractions and chlorophyll-a concentration. This investigation of variability was done with the size-fractionated chlorophyll-a data.

Our data suggest that the a_{LH}*is positively related to the fraction of F_{small} phytoplankton in the water, with a higher a_{LH}* associated with a higher proportion of small cells (Fig. 5(B)). This is most clearly seen in the spring 2021 where there was a higher proportion of large cells and a_{LH}* values were lower compared to the other cruises, suggesting that changes in community composition affected a_{LH}*. This agrees with other studies, that have shown that lower a_{LH}* values can result from an increase in cell size or intracellular pigment concentrations, which both lead to an increase in pigment packaging within the cell [12]. Where increased pigment per cell volume, increases the packaging effect causing the flattening of the relationship between a_{LH} and chlorophyll-a, decreasing a_{LH}* (Fig. 5(D)). Summer 2020, fall 2020 and summer 2021 all had a larger proportion of small cells, thus their a_{LH}* values were higher than spring 2021.

Environmental light conditions also impact pigment packaging, where at high light levels, cells can increase their packing effect (photoacclimation) to avoid production of oxygen radicals, thereby decreasing a_{LH}* values [12]. We suggest that the variation in a_{LH}* between summer 2020 and summer 2021 is due to environmental conditions. Where the median density was lower (Fig. 3(A)), the PAR was higher (Fig. 3(B)) and the diffuse attenuation coefficient lower for summer 2020 than summer 2021. This suggest that summer 2020 had a less stratified water column that had more light which attenuated slower, so phytoplankton in summer 2020 were exposed to higher light levels which might explain the lower in a_{LH}* in summer 2020, compared to summer 2021. The higher light exposure could have led to increased photoacclimation, decreasing the a_{LH}* for the summer 2020 data set. In contrast, spring 2021 captured a large diatom bloom, with higher than average shelf values (2-30 µg/l with a mean of 6.5 µg/l compared to mean

Optics EXPRESS

concentrations between 2-8 µg/l from 1988-2011 remote sensing data). Blooms frequently lead to self-shading and low light adaptation within a phytoplankton community [28]. The median PAR of spring 2021 is lower at depth and that the mean density profile is close to vertical, suggesting the waters were well mixed (Fig. 3). This means that phytoplankton are exposed to lower light conditions during the bloom than in other seasons. Under such conditions, phytoplankton would aim to maximize the amount of light they capture. This would lead to an upregulation of chlorophyll-a production to create more pigments with more light-harvesting regions [29,30], thus increasing the ability to photosynthesize with limited light. This adaptation would drive elevated levels of pigment packaging, decreasing the a_{LH}*.

Seasonality may be an indicator of changes in other underlying variables. As discussed above, pigment packaging is driven by a variety of physiological traits. Temporal variations in a_{LH}* may be caused by a combination of phytoplankton physiology and environmental parameters that induce changes in physiological traits. Further studies on how community composition, stratification, and/or nutrient availability affect a_{LH}* may shed additional light on the underlying drivers of a_{LH}*. More data is needed to confirm whether we can establish regionally tuned seasonal values.

5. Conclusion

The initial motivation to collect the data presented here was to calculate a regionally tuned a_{Lh} value for the NGA. Our results showed that the NGA has comparable values to productive higher latitude coastal regions in the spring and open ocean regions in the summer. The results from this study support the importance of regionally tuned regressions for the LHA method, and it also shows that accounting for temporal variability in the LHA method is important. As such, the mean NGA value of 0.0114 that is presented should be treated with caution as there is temporal variability which could result in 25.6% error when estimating chlorophyll-a in the region. This temporal variability is critical in regions where environmental conditions and/or community composition change. To minimize potential errors when applying the LHA method, we suggest checking whether there is a temporal change in a_{LH}* in your region of interest. This work also confirms that the LHA method is robust in a variety of waters, including glacial flour waters and high chlorophyll-a waters (>20 µg chl/L). Future work could investigate whether the seasonal pattern in a_{LH}* persists across multiple years and in other regions, along with investigating which underlying physical and environmental factors affect a_{LH}* leading to the observed seasonality.

Funding. Gordon and Betty Moore Foundation (11171); National Aeronautics and Space Administration (21-OCEANstep2-0018); North Pacific Research Board (2001).

Acknowledgments. We would like to thank the captains and crew of the R/V Sikuliaq for navigating both rough and calm waters so that we could continue to sample. We would like to thank the NGA-LTER program for their support. We would like to thank the members of the Rivero-Calle Lab for many fruitful conversations and feedback during the analysis and writing of the manuscript and the Skidaway Institute of Oceanography for providing the startup funds to support BL and SRC during this process. We would like to thank the reviewers for their helpful and many comments, which led to an improved manuscript.

Disclosures. The authors declare no conflicts of interest.

Data availability. The data produced by this work are archived and publicly available on PANGAEA in Refs. [31, 32, 33, 34]. The Data is further publicly available through Research Workspace, under the Northern Gulf of Alaska Long Term Ecological Research Site (NGA LTER).

Supplemental document. See Supplement 1 for supporting content.

References

1. C. S. Roesler and A. H. Barnard, "Optical proxy for phytoplankton biomass in the absence of photophysiology: Rethinking the absorption line height," Methods in Oceanography **7**, 79–94 (2013).
2. C. Hu, Z. Lee, and B. Franz, "Chlorophyll-a algorithms for oligotrophic oceans: A novel approach based on three-band reflectance difference," J. Geophys. Res.: Oceans **117**(C1), 1 (2012).

Optics EXPRESS

3. E. Boss, M. Picheral, T. Leeuw, *et al.*, "The characteristics of particulate absorption, scattering and attenuation coefficients in the surface ocean; Contribution of the Tara Oceans expedition," Methods in Oceanography **7**, 52–62 (2013).
4. L. Deng, W. Zhou, W. Cao, *et al.*, "Retrieving Phytoplankton Size Class from the Absorption Coefficient and Chlorophyll A Concentration Based on Support Vector Machine," Remote Sens. **11**(9), 1054 (2019).
5. W. J. Burt, T. K. Westberry, M. J. Behrenfeld, *et al.*, "Carbon: Chlorophyll Ratios and Net Primary Productivity of Subarctic Pacific Surface Waters Derived From Autonomous Shipboard Sensors," Global Biogeochem. Cycles **32**(2), 267–288 (2018).
6. H. F. Houskeeper, D. Draper, R. M. Kudela, *et al.*, "Chlorophyll absorption and phytoplankton size information inferred from hyperspectral particulate beam attenuation," Appl. Opt. **59**(22), 6765–6773 (2020).
7. C. Minaudo, D. Odermatt, D. Bouffard, *et al.*, "The Imprint of Primary Production on High-Frequency Profiles of Lake Optical Properties," Environ. Sci. Technol. **55**(20), 14234–14244 (2021).
8. E. Organelli, H. Claustre, A. F. Bricaud, *et al.*, "Bio-optical anomalies in the world's oceans: An investigation on the diffuse attenuation coefficients for downward irradiance derived from Biogeochemical Argo float measurements," Journal of Geophysical Research: Oceans **122**(5), 3543–3564 (2017).
9. M. Barbieux, J. Uitz, A. Bricaud, *et al.*, "Assessing the Variability in the Relationship Between the Particulate Backscattering Coefficient and the Chlorophyll a Concentration From a Global Biogeochemical-Argo Database," J. Geophys. Res.: Oceans **123**(2), 1229–1250 (2018).
10. Z. Lee, J. Marra, M. J. Perry, *et al.*, "Estimating oceanic primary productivity from ocean color remote sensing: A strategic assessment," Journal of Marine Systems **149**, 50–59 (2015).
11. M. Werther, D. Odermatt, S. G. H. Simis, *et al.*, "A Bayesian approach for remote sensing of chlorophyll-a and associated retrieval uncertainty in oligotrophic and mesotrophic lakes," Remote Sensing of Environment **283**, 113295 (2022).
12. S. C. Nardelli and M. S. Twardowski, "Assessing the link between chlorophyll concentration and absorption line height at 676 nm over a broad range of water types," Opt. Express **24**(22), A1374–A1389 (2016).
13. C. S. Yentsch and D. A. Phinney, "A bridge between ocean optics and microbial ecology," Limnol. Oceanogr. **34**(8), 1694–1705 (1989).
14. A. Bricaud, M. Babin, A. Morel, *et al.*, "Variability in the chlorophyll-specific absorption coefficients of natural phytoplankton: Analysis and parameterization," J. Geophys. Res.: Oceans **100**(C7), 13321–13332 (1995).
15. A. R. Childers, T. E. Whitledge, and D. A. Stockwell, "Seasonal and interannual variability in the distribution of nutrients and chlorophyll a across the Gulf of Alaska shelf: 1998–2000," Deep Sea Res., Part II **52**(1-2), 193–216 (2005).
16. P. R Mundy, (2005). *The Gulf of Alaska: Biology and oceanography. Alaska Sea Grant College Programm*, Univ. of Alaska Fairbanks.
17. J. N. Waite and F. J. Mueter, "Spatial and temporal variability of chlorophyll-a concentrations in the coastal Gulf of Alaska, 1998–2011, using cloud-free reconstructions of SeaWiFS and MODIS-Aqua data," Prog. Oceanogr. **116**, 179–192 (2013).
18. S. Strom, M. Olson, E. Macri, *et al.*, "Cross-shelf gradients in phytoplankton community structure, nutrient utilization, and growth rate in the coastal Gulf of Alaska," Mar. Ecol. Prog. Ser. **328**, 75–92 (2006).
19. T. R. Parsons, Y. Maita, and C. M. Lalli, *A Manual of Chemical and biological methods for seawater analysis* (1st ed.). (Pergamon Press., 1984).
20. Seth Danielson. Hydrographic, optical, and meteorological parameters measured by R/V Sikuliaq's underway systems during the Northern Gulf of Alaska LTER cruises, 2018- 2021. DataOne. https://doi.org/10.24431/rw1k45a . Version: 10.24431_RW1K45A_20230220T205044Z. Accessed on August 10th, 2023. (2023).
21. W. O. Smith Jr and R. M. Jones, "Vertical mixing, critical depths, and phytoplankton growth in the Ross Sea," ICES J. Mar. Sci. **72**(6), 1952–1960 (2015).
22. J. M. Sullivan, M. S. Twardowski, J. R. V. Zaneveld, *et al.*, "Hyperspectral temperature and salt dependencies of absorption by water and heavy water in the 400-750 nm spectral range," Appl. Opt. **45**(21), 5294–5309 (2006).
23. Sea-Bird Scientific. Spectral Absorption and Attenuation Sensor (ac-s) User's Guide. Revision M. (2013).
24. E. Boss, N. Haëntjens, Ackleson, *et al.*, IOCCG, Dartmouth, NS, Canada. (2019).
25. B. J. Pan, M. Vernet, R. A. Reynolds, *et al.*, "The optical and biological properties of glacial meltwater in an Antarctic fjord," PLoS ONE **14**(2), e0211107 (2019).
26. M. Babin, J.-C. Therriault, L. Legendre, *et al.*, "Variations in the specific absorption coefficient for natural phytoplankton assemblages: Impact on estimates of primary production," Limnol. Oceanogr. **38**(1), 154–177 (1993).
27. M. E. Ondrusek, R. R. Bidigare, K. Waters, *et al.*, "A predictive model for estimating rates of primary production in the subtropical North Pacific Ocean," Deep Sea Res., Part II **48**(8-9), 1837–1863 (2001).
28. S. L. Strom, K. A. Fredrickson, and K. J. Bright, "Spring phytoplankton in the eastern coastal Gulf of Alaska: Photosynthesis and production during high and low bloom years," Deep Sea Res., Part II **132**, 107–121 (2016).
29. P. G. Falkowski and J. LaRoche, "Acclimation to Spectral Irradiance in Algae," J. Phycol. **27**(1), 8–14 (1991).
30. N. H. Hintz, B. Schulze, A. Wacker, *et al.*, "Ecological impacts of photosynthetic light harvesting in changing aquatic environments: A systematic literature map," Ecology and Evolution **12**(3), e8753 (2022).
31. B. Lowin and W. J. Burt, "Absorption, attenuation, scattering and backscattering inline data from the Gulf of Alaska in July 2020," PANGAEA 2023, https://doi.org/10.1594/PANGAEA.962680.

Optics EXPRESS

32. B. Lowin and W. J. Burt, "Absorption, attenuation, scattering and backscattering inline data from the Gulf of Alaska in September 2020," PANGAEA 2023, https://doi.org/10.1594/PANGAEA.962686.
33. B. Lowin and W. J. Burt, "Absorption, attenuation, scattering and backscattering inline data from the Gulf of Alaska in April/May 2021," PANGAEA 2023, https://doi.org/10.1594/PANGAEA.962687.
34. B. Lowin and W. J. Burt, "Absorption, attenuation, scattering and backscattering inline data from the Gulf of Alaska in June/July 2021," PANGAEA 2023, https://doi.org/10.1594/PANGAEA.962688.